Physics Letters A 380 (2016) 1189–1192

Contents lists available at ScienceDirect

Physics Letters A

www.elsevier.com/locate/pla

Mass number identification by Alfvén wave diagnostics in hydrogen and helium plasmas in TCABR

P.G.P. Puglia, A.G. Elfimov *, A.V. Andriati, R.M.O. Galvão, Z.O. Guimarães-Filho, G. Ronchi, L.F. Ruchko

Institute of Physics, University of São Paulo, Rua do Matão Travessa R, 187, São Paulo, 05508-090, Brazil

ARTICLE INFO

Article history:
Received 4 November 2015
Accepted 11 January 2016
Available online 21 January 2016
Communicated by F. Porcelli

Keywords:
Tokamak
Diagnostics
Global Alfvén wave
Impurity accumulation
Effective mass number

ABSTRACT

The mass number is obtained through the identification of the Global Alfvén (GA) wave resonances in ohmic plasma discharges in the TCABR tokamak. By comparing hydrogen and helium discharges, the composition of carbon, oxygen, and iron impurities is determined. The non-perturbative Alfvén diagnostic is used that is based on the excitation of GA waves by an external antenna fed by a low power generator, in the frequency band swept just below the minimum of the Alfvén wave continuum. Odd or even toroidal modes are excited by selecting the current phase in the two antenna modules separated by 180 degrees in the toroidal direction. The density profile, determined from cross analysis of reflectometer and interferometer data, shows impurity accumulation in the plasma core.

1. Introduction

In many regular tokamak discharges, an uncontrolled accumulation of high-Z ions in the plasma core has been observed [1]. This effect may lead to unacceptable radiative cooling, generate undesirable plasma instabilities leading to disruptions, as well, it may undermine the burning efficiency in ITER. A relevant task in fusion research is to control the impurity concentration in the confined plasma. Naturally, a first step in the problem is to measure the impurity concentration. However, measurement of the effective mass number, $A_{ef} = \sum_i n_i m_i / n_e m_H$, is not straightforward using standard tokamak diagnostics. One method, dubbed "MHD diagnostics", has been explored [2–6] to obtain information about both the mass number and q-profile. Specifically, Global Alfvén (GA) waves have been proposed to measure the effective mass number [2,3,7]. The Alfvén diagnostics is a non-perturbative method that uses the resonances of GA waves [7–9] excited by an external antenna fed by a low power generator, in a swept frequency mode, just below the minimum (or about the maximum [10]) of the Alfvén wave continuum that is determined from the radial component of Ampere's equation with MHD dielectric tensor, $c^2 k_{||}^2 = \sum_i \omega_{pi}^2 \omega^2 / (\omega_{ci}^2 - \omega^2)$, yielding the relation

$$\omega_A = \frac{c_A k_{||}}{\sqrt{1 + (c_A k_{||}/\omega_i)^2}}, \qquad k_{||} = \frac{B_t}{B_0 R_0}\left(N + \frac{m}{q(r)}\right),$$
$$c_A \approx \frac{B_0}{\sqrt{4\pi m_H A_{ef} n_e(r)}} \tag{1}$$

Here, ω_A is the Alfvén wave frequency, $k_{||}$ is the wave vector parallel to the magnetic field, c_A is the Alfvén speed, B_t is the toroidal magnetic field strength, n_e is the electron density, m_H is the hydrogen nuclei mass, R_0 is the major tokamak radius, (N, M) are the toroidal and poloidal wave numbers and q the safety factor.

For effective application of the method, it is necessary to know well the electron density profiles. In the case of TCABR, the standard density profile is of the parabolic type $\sim (1 - r^2/a^2)^\alpha$. However, recent experiments [11] show that impurity accumulation in the plasma core modifies the density profile, which acquires a "Mexican hat" shape. Inwardly directed drift velocities may cause impurity accumulation, which leads to peaked profiles of the effective charge number Z_{eff} [1], as well A_{eff}. The early-developed theory [12] predicts impurity accumulation when the electron density appears to be peaked in the form of a maxwellian radial distribution [12]

$$n_e \approx Z_i n_{0i}\left(1 - r^2/a^2\right)^\alpha + Z_Z n_{0Z} \exp\left(-r^2/\sigma^2 a^2\right) \tag{2}$$

where $n_{i,Z}$ is the density and $Z_{i,Z}$ is the charge of main or impurity ions, respectively. This distribution is valid for combined collisional and/or anomalous transport that is typical in Ohm's discharges in the TCABR tokamak [7,13]. We note that in this device

* Corresponding author. Tel.: +55 11 3091 6809.
E-mail address: elfimov@if.usp.br (A.G. Elfimov).

http://dx.doi.org/10.1016/j.physleta.2016.01.025
0375-9601/

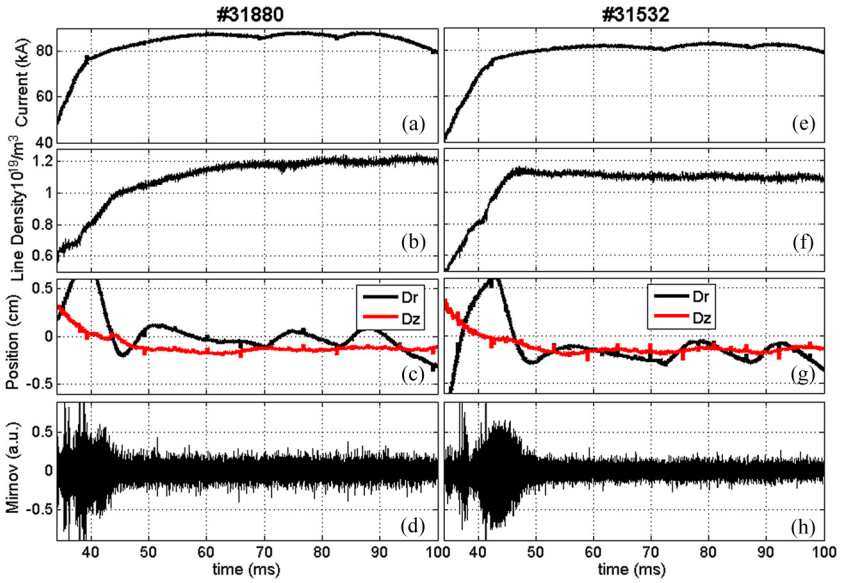

Fig. 1. Time evolution of basic plasma parameters for discharge #31880 and #31532, with helium and hydrogen. The signals shown are electron plasma current (a, e), central line density (b, f), horizontal and vertical plasma positions (c, g), and magnetic field oscillations (d, h).

the main sources of impurity are the carbon from the limiter and iron from the chamber.

Here, using the Alfvén diagnostics equipment described in Ref. [7] in combination with O-mode reflectometer and interferometer measurements [13,14] of the electron density profile, we study the effective mass number variation in helium plasmas in comparison with hydrogen ones in Ohm's discharges in TCABR. The discharges are performed in regimes with saw tooth oscillations that help us to define the $q = 1$ position, which is necessary information to define the GAW frequency at the plasma core.

2. Experimental results

The main parameters of the TCABR tokamak are major radius $R_0 = 0.615$ m, minor radius $a = 0.18$ m, toroidal magnetic field $B_0 = 1.07$ T, range of plasma current $I_P = 78$–90 kA, with central electron temperature around $T_{e0} \approx 500$–550 eV, for hydrogen and 550–600 eV for helium plasmas, measured by Thomson scattering and central line averaged electron density $\bar{n} = 1.0$–1.5×10^{19} m^{-3}. The GA wave are excited by two antennae, which are 180° toroidally separated, with RF currents powered by two low power RF amplifiers $P_{RF} < 0.5$ kW, whose phases are equal [0–0] or opposite [0–π] to allow launching waves with even or odd toroidal mode numbers. All discussed shots are accompanied by saw tooth oscillation with inversion radius at $r \approx 3.5 \pm 1$ cm, detected by Soft-X Ray diagnostics. That information, supplemented by the value of the edge safety factor, is used to reconstruct the current profile as $j_{oh} = j_0(1 - r^2/a^2)^{\alpha j}$, where $\alpha_j = 2.5$–2.6 during the stable part of the discharge, i.e., without strong magnetic perturbations registered by Mirnov coils in the time interval $t = 45$–100 ms. In Fig. 1, the time evolution of the basic plasma parameters is shown for discharges #31880 (helium) and #31532 (hydrogen) as typical examples of discharges that are used for the Alfvén diagnostic experiments.

In previous TCABR experiments [7], two lines of the interferometer were used to identify the core density, based upon the standard parabolic-in-power density profile $\propto (1 - r^2/a^2)^{\alpha}$, with $\alpha \approx 1$–1.5, and Shafranov shift $\Delta R = \delta(1 - (R - R_0)^2/a^2)$ with $\delta = (\beta_{\rm pol} + 1/4)a^2/2R_0 \approx 1 - 1.5$ cm. In these experiments, the second interferometer channel was not available, so that we determined the density profile using the group delay signal of the reflectometer and the central line density of the interferometer. Standard spectrograms of signals of the O-mode reflectometer [14], in the K and Ka frequency bands (18–42 GHz), which are swept during 8 μs and repeated every 15 μs, are used to build the group delay signal shown in Fig. 2a, b. Then, using the theoretically predicted density profile (2) $n_e = n_0[(1 - r^2/a^2)^{\alpha} + \beta \exp(-r^2/\sigma^2 a^2)](1 + \beta)^{-1}$, the experimental group delay signal is adjusted by the calculated τ_g-value, $\tau_g = (2a/c)\int_{xr}^{1} dx/\sqrt{1 - f_p^2(x)/f^2}$, where $x = (R - R_0)/a$, $f_p(x) = 8.98 \cdot 10^3\sqrt{n_e(x)}$ Hz is the local plasma frequency and x_r is reflection point. In the reported low-density discharges, the evaluated density profile appears to be peaked with $\alpha \approx 1.6$ for Hydrogen and $\alpha \approx 1.92$ for Helium. The higher peaking parameter $\sigma \approx (0.23 \pm 0.03)a$ for small accumulation of impurity $\beta = Z_Z n_{0Z}/n_{0e} \approx 0.20$–$0.24$ is observed in all discharges.

The calculated density profile from reflectometer data is cross-checked with the interferometer data, using a Shafranov shift about of 1.–1.3 cm to obtain the central density. The resulting value shows good agreement with interferometer data previously taken with two line-of-sight positions, $R - R_0 = -1.25$ and 9.25 cm, in a series of different shots, which were selected as identical during the stationary part of the discharges in the interval 50–100 ms. It has been found that the density maximum $n_{\max}$ defined by the reflectometer cut off signal systematically stays below the interferometer one by 3–4%, value with a 5% standard deviation.

To detect the magnetic field oscillations excited by the Global Alfvén Eigenmode, we use one magnetic probe located between the two antennae, in the toroidal direction, and in the shadow of the limiter. The probe is placed at the bottom of the chamber at the low field side, in an angular position shifted by ∼45° from equatorial plane in relation of the chamber center. Initially, in the data analyses, we calculate the spectrogram of the magnetic signals and get the spectral power at the frequency of the RF current, using the synchronizing signal for both the RF current and magnetic probes.

The treated probe signals for discharges #31880 (helium) and #31532 (hydrogen) are presented in Fig. 3(a, b), for the corresponding integrated spectral power around the RF frequency during sweeping in the band ($f = 2.0$–3.6 MHz). In these figures, we may observe high spikes, which are identified as resonances of the mode numbers $N/M = 2/1$ driven by [0, 0] phasing of the antenna currents. That data will be used for comparing the effective mass of the shots.

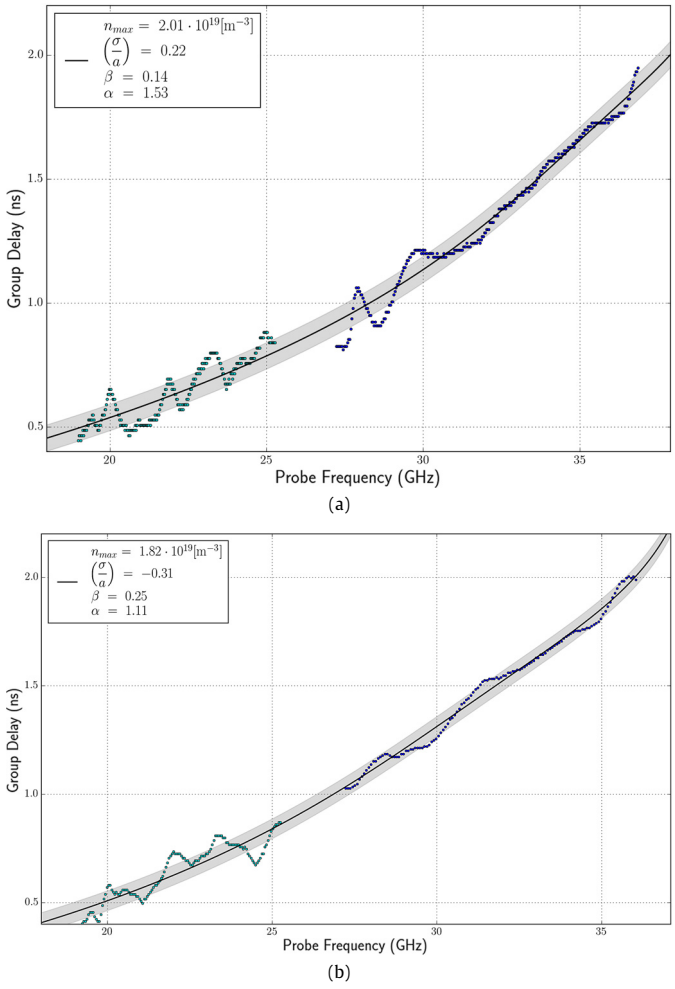

Fig. 2. Group delay of the reflectometer signal (black points) and calculated value (solid line, shadowed by standard deviation error) using density profile in eq. (2) (a) for the helium discharge #31880 at the detected resonance moment $t = 71.2$ ms and 81 ms; (b) for the hydrogen discharge #31532 at the detected resonance moment 81.2 ms.

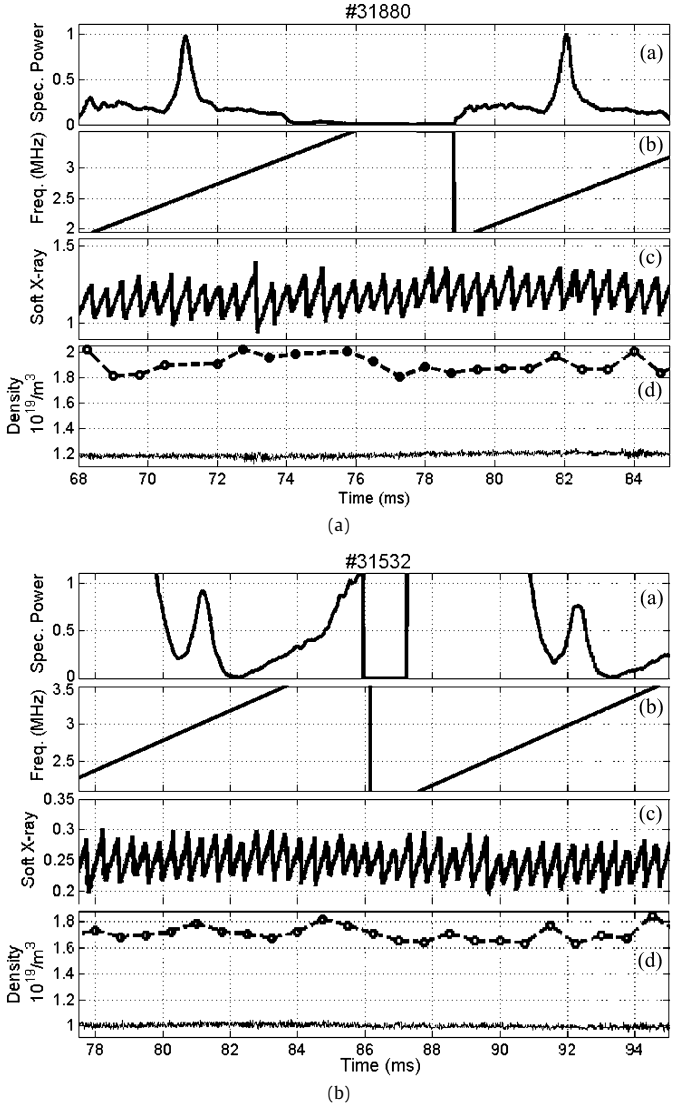

Fig. 3. Time traces (from top to bottom) of the spectral power of the probe signals normalized by the RF current in comparison with the frequency sweeps (2d window) of the RF antenna current, the soft X-ray signal (3d window) and the central density found from the reflectometer together with the line averaged electron plasma density (a) in the helium plasma discharge #31880; (b) in the hydrogen plasma discharge #31532.

In Fig. 4, we summarize all the found resonances in helium discharges and show their dependence from the core line density, with a 5% deviation error band. The lower mode is identified as the global Alfvén wave with the toroidal/poloidal mode numbers $N/M = 2/1$. The detected modes present the behavior expected from eq. (1), i.e., show decreasing resonant frequencies as the density increases $\propto 1/\sqrt{A_{ef} n_0}$. As we are comparing the frequency of the modes with the integrated line density, the relation between the two values is not as smooth as it shown in previous work [7], where the estimation of the core plasma density was somewhat better.

3. Discussion

The general dependence of the GAW resonance frequency on the central line density stays in accordance with Eq. (1), but it should be corrected for the dependence on the $A_{ef} n_0$-parameter. First, we recalculate the electron density maximum using cross data from the reflectometer/interferometer measurements. In particular, we find $n_{0eHe} = 1.95 \cdot 10^{19}$ m^{-3} for the helium and $n_{0eH} = 1.85 \cdot 10^{19}$ m^{-3} for hydrogen plasmas, shown at the first resonance conditions in Figs. 3(a) and 3(b), respectively. Then, using the GAW resonance frequencies 2.5 MHz and 3.1 MHz shown in these figures, we calculate the effective mass numbers $A_{He} = 2.07 \pm 0.05$ for helium and $A_H = 1.49 \pm 0.07$ for hydrogen plasmas, respectively. As it has been discussed in previous study [7], the hydrogen plasmas are diluted by $n_{lt}/n_e \approx 6\%$ of light impurities (carbon + oxygen) and $n_{Fe}/n_e \approx 0.15\%$ of the Fe_{56}^{+17}-impurity, satisfying the effective charge $Z_{ef} \approx 3.1$. In this series of the hydrogen discharges, the level of impurities is estimated to be slightly higher corresponding to 6.5% of light impurities with the effective charge $Z_{ef} \approx 3.2$. Comparing this data with the helium discharges, which has $Z_{ef} \approx 4$, and assuming that the carbon is fully ionized and the Fe-impurity has the same ionization level Fe_{56}^{+17}, we estimate a 1% concentration of O_{16}^{+7}, which level of ionization corresponds to $T_e \approx 600$ eV, complying with the figure previously determined in the TFR tokamak [15]. We note that the mass number estimations found for the discharges #31880 and #31532 are the same for all discharges in the line density interval $0.9–1.5 \cdot 10^{19}$ m^{-3} shown in Fig. 4, where the density maximum may be definitely detected with the interferometer/reflectometer measurements.

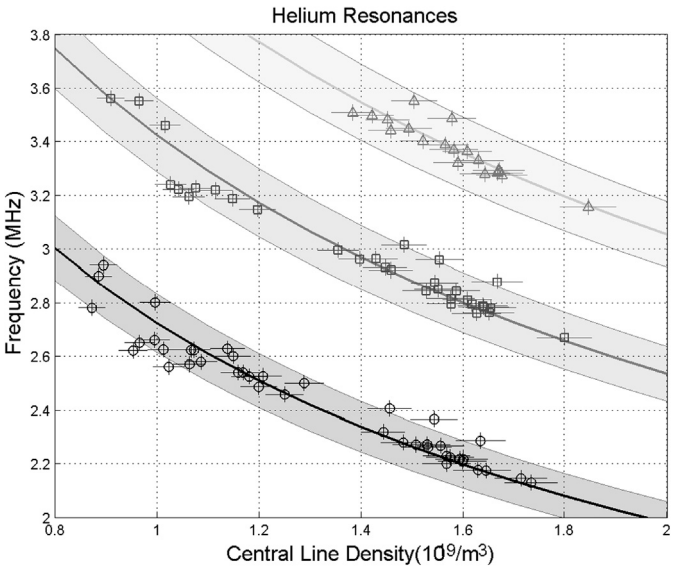

Fig. 4. Dependence of identified resonant frequencies from the estimated core density for modes $|N| + |M| = 3$ (circles), 4 (squares) and 5 (triangles). The lowest spectrum represents the $N/M = 2/1$ mode.

4. Conclusion

Using the Alfven wave diagnostics together with interferometer and reflectometer density measurements, the effective mass numbers are found for the helium and hydrogen plasma discharges in the TCABR tokamak. The general dependence of the global Alfvén wave frequency is confirmed to be proportional to the square root of the inversed mass density $\propto 1/\sqrt{A_{ef} n_0}$ in these discharges. Strong density peaking of the density profile is observed due to impurity accumulation that is mainly composed by carbon impurity (≈5–5.5%) with small account for oxygen (≈1%) and iron (≈0.15%).

Acknowledgements

This work was supported by FAPESP (Research Foundation of the State of São Paulo), contract 2011/50773-0, and by CNPq (National Council of Scientific and Technological Development) contracts 480733/2013-9 and 307511/2011-1, Brazil.

References

[1] R. Dux, Fusion Sci. Technol. 44 (2003) 708.
[2] G.A. Collins, A.A. Howling, J.B. Lister, P. Marmillod, Plasma Phys. Control. Fusion 29 (1987) 323.
[3] P. Descamps, G. Wassenhove, R. Koch, A.M. Messiaen, P.E. Vandenplas, Phys. Lett. A 143 (1990) 311.
[4] A. Fasoli, A. Dobbing, C. Gormezano, J. Jacquinot, J.B. Lister, S.E. Sharapov, A. Sibley, Nucl. Fusion 36 (1996) 258.
[5] H.A. Holties, A. Fasoli, J.P. Goedbloed, G.T.A. Huysmans, W. Kerner, Phys. Plasmas 4 (1997) 709.
[6] A.G. Elfimov, L.F. Ruchko, R.M.O. Galvão, J.I. Elizondo, E. Sanada, M.E.C. Manso, P. Varela, A. Silva, A.A. Ivanov, Nucl. Fusion 46 (2006) S722.
[7] P.G.P. Puglia, A.G. Elfimov, L. Ruchko, R.M.O. Galvão, Z.O. Guimarães-Filho, G. Ronchi, Phys. Plasmas 21 (2014) 122509.
[8] K. Appert, R. Gruber, F. Troyuon, J. Vaclavik, Plasma Phys. Control. Fusion 24 (1982) 1147.
[9] D.W. Ross, G.L. Chen, S.M. Mahajan, Phys. Fluids 25 (1982) 652.
[10] A.G. Elfimov, R.M.O. Galvão, S.E. Sharapov, Phys. Plasmas 17 (2010) 110705.
[11] T. Nicolas, R. Sabot, X. Garbet, H. Lütjens, J.-F. Luciani, A. Sirinelli, J. Decker, A. Merle, JET-EFDA Contributors, J. Plasma Fusion Res. 8 (2013) 2402131.
[12] G. Fussmann, A.R. Field, A. Kallenbach, K. Krieger, K.-H. Steuer, ASDEX Team, Plasma Phys. Control. Fusion 33 (1991) 1677.
[13] R.M.O. Galvão, C.H.S. Amador, W.A.H. Baquero, et al., J. Phys. Conf. Ser. 511 (2014) 012001.
[14] A.M.M. Fonseca, S. Hacquin, R.M.O. Galvão, J.I. Elizondo, P.G. Puglia, L.F. Ruchko, C. Amador, J.C. Raffaelli, J.H.F. Severo, I.C. Nascimento, J. Phys. Conf. Ser. 511 (2014) 012006.
[15] C. Breton, C. de Michelis, M. Mattioli, Nucl. Fusion 16 (1976) 891.